Electronic Supplementary Material (ESI) for RSC Advances.

SUPPORTING INFORMATION

Synthesis and Characterization of Carbosilane Dendrimer−Sodium Montmorillonite Clay Nanocomposites. Experimental and Theoretical Studies

Tomáš Strašák[a,b*], Marek Malý[b*], Monika Müllerová[a], Jan Čermák[a,c], Martin Kormunda[b], Pavla Čapková[b], Jindřich Matoušek[b], Lucie Červenková Šťastná[a], Jaroslav Rejnek[c], Jana Holubová[d], Věra Jandová[a], Klára Čépe[e]

[a]Institute of Chemical Process Fundamentals of the CAS, v.v.i, Prague, Czech Republic

[b]Department of Physics, Faculty of Science, University of J.E. Purkinje, Usti N/L, Czech Republic

[c]Department of Chemistry, Faculty of Science, University of J.E. Purkinje, Usti N/L, Czech Republic

[d]Department of General and Inorganic Chemistry, University of Pardubice, Pardubice, Czech Republic

Table S1. XRD results of prepared organoclays.

	2Ø[degrees]	*d*-spacing [Å]
0.1Dm1Mt	5.79	15.3
0.2Dm1Mt	5.85	15.1
0.5Dm1Mt	5.91	14.9
0.1Dm2Mt	5.85	15.1
0.2Dm2Mt	5.9 - 5.2	15 - 17.0
0.5Dm2Mt	4.48	19.7
Na-Mt	7.17	12.5

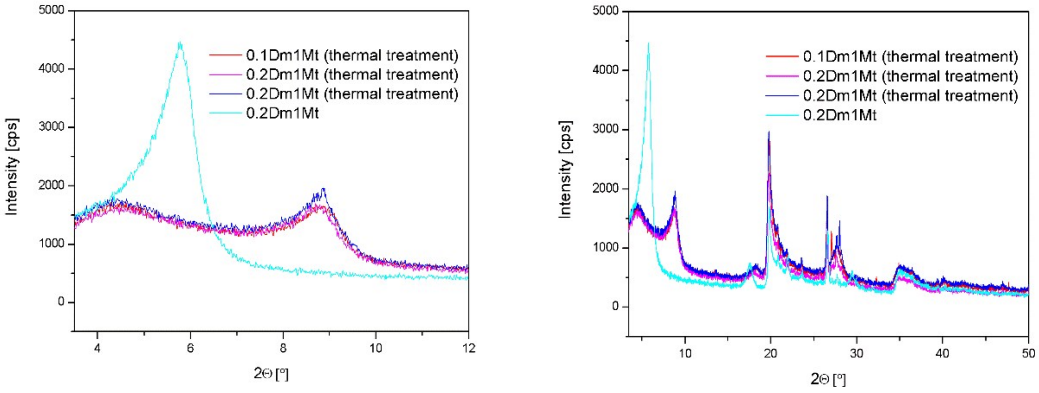

Figure S1. X-ray diffractograms of the basal reflections of montmorillonite intercalated by dendrimers **Dm1** after thermal oxidation (10 °C/min to 700 °C in air). Untreated sample **0.2Dm1Mt** is presented for comparing.

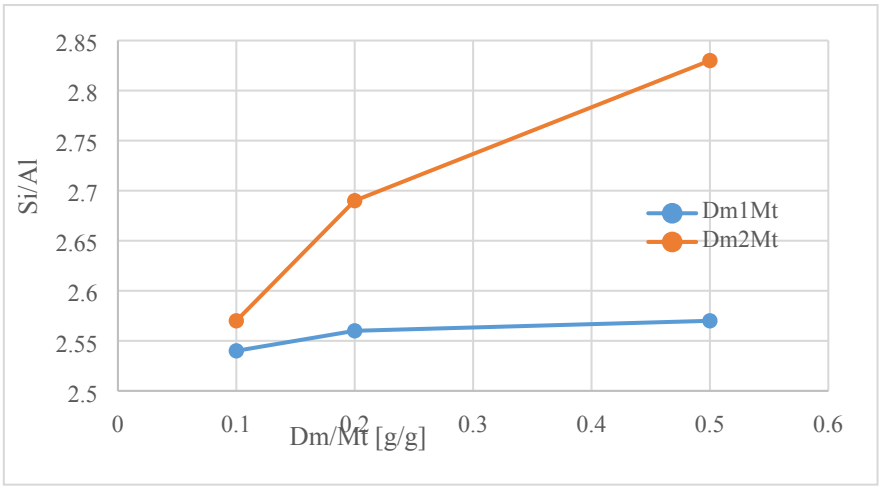

Figure S2. Results of EDX for **Dm1Mt** and **Dm2Mt.**

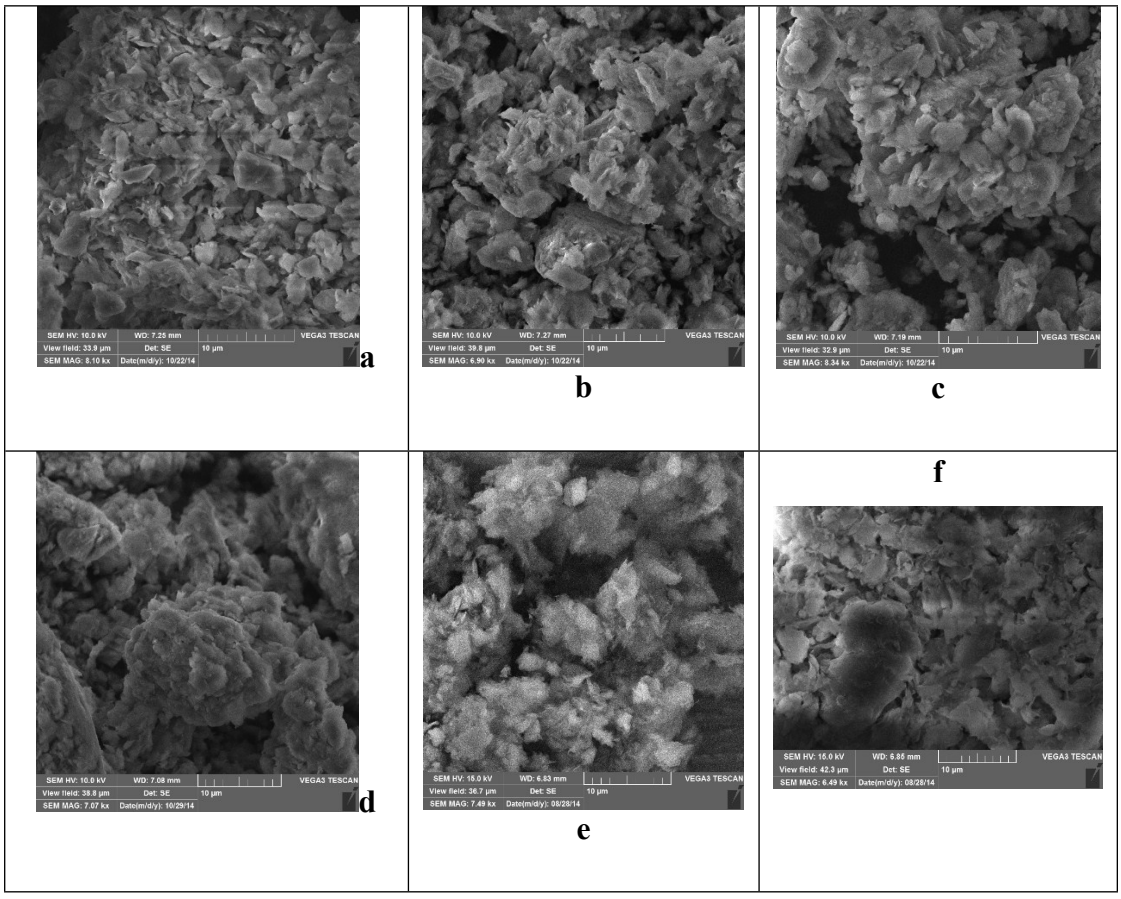

Figure S3. SEM images of **0.1Dm1Mt** (a), **0.2Dm1Mt** (b), **0.5Dm1Mt** (c), **0.1Dm2Mt** (d), **0.2Dm2Mt** (e) and **0.5Dm2Mt** (f).

Molecular modeling

Methods

Computer models of Dendrimer (D)/Montmorillonite (Mt) systems were created and simulated using Materials Studio from BIOVIA (formerly Accelrys). Dendrimers were created using polymer builder and the Mt layers were obtained as the supercell, based on unit cell structure with registration number 9002779 (Triclinic lattice type, symmetry space group P1, a = 5.18 Å, b = 8.98 Å, c = 15 Å, α=90°, β =90°, γ =90°) deposited in Crystallography Open Database [1] which was replicated in **a** (9 x) and **b** (5 x) directions. Chemical formula of the Mt structure 9002779 is $Al_2\ Ca_{0.5}\ O_{12}\ Si_4$ (composition formula reflecting actual number of atoms in the given structure $Al_4\ Ca\ O_{24}\ Si_8$). The final single Mt layer has dimensions 46.62 Å × 44.9 Å . This way we obtained template for computer model of Mt structure. The original composition of Mt used in our experiments is given by chemical formula:

$(Si_{4.0})\ (Al_{1.45}Fe^{3+}_{0.21}Mg_{0.24}Ti_{0.01})\ K_{0.07}Na_{0.25}Ca_{0.10}\ O_{10}(OH)_2$. As we can clearly see from this experimentally obtained composition, there are just "Al" substitutions or vacancies. If there were also some "Si" substitutions in the analysed Mt samples, they were under detection limit. Unfortunately the negative charge of the Mt layer which is compensated by K^+,Na^+ and Ca^{++} cations, is here not only due to the substitutions of Al^{3+} by Mg^{2+} or Ti^{2+} but also due to some vacancies in the ideal structure as 1.45 + 0.21 + 0.24 + 0.01 = 1.91 (not 2 as in ideal structure). So the total charge of the layer or more precisely charge of the half of the unit cell given by the above formula (without cations) Q= (1.45*3 + 0.21*3 +0.24*2+0.01*2) – 2*3 = -0.52 is composed of (1.91-2)×3 = -0.27 charge resulting from vacancies (missing Al atoms without any substitution) and the rest (-0.25) resulting from substitutions of Al atoms by elements in oxidation state 2+. So in the real case the 46.62 Å × 44.9 Å part of one layer surface (without free cations) should carry 2×45*(-0.52) = -46.8 charge, where –24.3 should be charge resulting from vacancies. In our case the real Mt composition: $(Si_{4.0})\ (Al_{1.45}Fe^{3+}_{0.21}Mg_{0.24}Ti_{0.01})\ K_{0.07}Na_{0.25}Ca_{0.10}\ O_{10}(OH)_2$ (after the small simplification $Mg_{0.24}Ti_{0.01}$ -> $Mg_{0.25}Ti_{0.00}$) was mapped on 46.62 Å × 44.9 Å ideal supercell given by formula $Si_{4.0}Al_2\ O_{10}(OH)_2$ (structure 9002779 i.e. without any vacancies) therefore the total layer charge was only –24. To obtain realistic charge (-47) there was necessary to increase the number of Mg^{2+} substitutions of 23 to compensate lack of vacancies. We decided to substitute all 20 Fe atoms, which is the number corresponding to ideal supercell 46.62 Å × 44.9 Å after the mapping the experimental formula on it, and 3 Al atoms. This decision was motivated mainly by the fact, that there is missing proper atom type for Fe in 3+ oxidation state in Universal force field which we used for the subsequent simulations. Of course, at the end the

proper amount of cations was added to obtain neutral system, so the chemical formula of the final computer model was:

$(Si_{4.0})\ (Al_{1.478}Fe^{3+}{}_{0.0}Mg_{0.522}Ti_{0.0})\ K_{0.067}Na_{0.256}Ca_{0.10}\ O_{10}(OH)_2$.

Partial charges of montmorillonite and dendrimer atoms were calculated using Charge Equilibration Method (QEq) [2]. In case of water we used charges from SPC/E water model (i.e −0.8476 for O and +0.4238 for H) as with this charges the density of bulk water is significantly better reproduced than in case of Qeq charges. Universal force field was used for all components (Mt, dendrimers, water). The 3D periodic systems composed of two Mt layers, ions, water molecules and dendrimers were prepared (see Fig. S4). The number of water molecules between the two Mt layers was set to 190 in case of simulation of pristine Mt (i.e. without dendrimers). This number was chosen because with this water amount, the interlayer distance obtained from our simulation (12.31 Å) corresponded well to the results obtained from our X-ray analysis (12.5 Å) of the real Mt material. Corresponding mass ratio mr = mass (H_2O)/mass (Mt sheets) 0.102 for this spacing is also in good agreement with results reported in another works [3, 8]. In case of systems containing dendrimers we at the end decided to reduce water content in Mt in dependence on number and generation of dendrimers in interlayer spaces which increased the agreement with experimental data. Our estimate of the water content in Mt in presence of dendrimers is based on approximative assumption that during the process of intercalation in water solution the dendrimers substitute water of the same volume as is the volume of dendrimers. This model evidently requires that during the intercalation process i) the average water density in Mt interlayer space and ii) volume of the interlayer space so hence d-spacing do not change. We assume that in situation of the high water content in Mt interlayer space (in contrary to low-water content case) both conditions are satisfied with sufficient precision for the amounts of dendrimers which goes inside the Mt using our intercalation procedure/protocol. If we add the last assumption, that the presence of dendrimers do not affect the relative amount of the water evaporated during the drying process, we can calculate the mass of remaining water content in concrete D-Mt system as follows: $M'_2 = M'_1 - M'_1/ M_1 * N_D * V_D * \rho = M'_1 - mr'_1/ mr_1 * N_D * V_D * \rho$ where M'_1 is the mass of remaining (after drying process) water in Mt interlayer space in case without dendrimers - i.e. known amount of water used for simulation of the pristine Mt - in our case mass of 190 H_2O molecules, M_1 is the mass of the water in interlayer space in case of high water content, N_D is number of dendrimers in the given interlayer space, V_D is dendrimer volume, ρ is the average water density in interlayer space in high water content case and mr_1, mr'_1 are water/(Mt sheets) mass ratios for high, low water content case in absence of dendrimers - see

figure S8. The dendrimers volumes were calculated as the volumes defined by the Connolly molecular surfaces where the typical "water-probe" radius 1.4 was used (vdW scale factor: 1, Connolly radius: 1.4). Lets just note, that the chosen "high water content case" might be here any such case which appears during the D-Mt composite preparation so also even if dendrimers in reality during the first steps adsorbs rather on the surfaces of free isolated Mt platelets which later reassemble in intercalated Mt. According to Hawkins and Egelstaff [8], the mr corresponding to 100% relative humidity is around 0.3. For our calculations we used mr_1 = 0.325 as according to above work at this water content the d-spacing reaches it's maximal value (ca 18.75 Å) or more precisely beginning of the last plateau part of the d-spacing dependence on mr. Our original used estimate for average water density ρ in such high hydration case was the density of bulk water under normal conditions i.e. 1000 kg/m^3. Later we found that for this mr the density will be slightly higher (around 1100 kg/m^3) [9]. The ρ estimate based on direct calculation of water accessible volume in Mt interlayer space for the given water content, using known d-spacing, width of Mt platelet and vdw "offsets" confirms this slight increase in density for mr_1 = 0.325 comparing to bulk water. As already mentioned above, mr'_1 = 0.102 (mass of 190 H_2O molecules divided by the mass of one platelet from our Mt model). Since used dendrimers are cationic (D1 charge = +4 , D2 charge = +8) the number of free cations (Na^+, K^+, Ca^{++}) in Mt/Dendrimer systems was adequately reduced to keep the final molecular systems neutral. The simulation protocol was as follows: First the initial positions of the Na^+, K^+, Ca^{++} cations, water molecules and dendrimer positions and conformations were optimised using "smart" algorithm (cascade of the steepest descent, adjusted basis set Newton-Raphson and quasi-Newton methods) [4] max. 5000 steps, convergence threshold 0.001 kcal/mol, the Ewald summation method [5] was used for computing of both, electrostatic and Van der Waals interactions, accuracy 0.0001 kcal/mol, repulsive cutoff (vdw) 6 Å. In exactly the same way were treated both non-bond interactions also in all remaining steps of our simulation protocol. Positions of all the Mt layer atoms (Si, Al, Mg …), except the internal OH groups, were fixed. Fixing and in later stage restraining of the Mt layer atoms was necessary as we found that Universal force field in combination with QEq charges is not able to maintain precisely the original crystal structure (given by unit cell 9002779) and some small (but not negligible) deformations appeared when additional fixing mechanisms was not used. The second step was 40 ps of NVT molecular dynamics simulation (still with fixed positions of the internal Mt atoms, T = 298 K, Nosé-Hoover thermostat used, time step 1 fs) [6]. After this step all the positional constraints were deleted (i.e. position of Mt atoms were no more fixed) instead the all Si-Si distances between Si atoms from opposite Si

surfaces (within the given Mt platelet) were restrained using harmonic restraints with force constant 2000 kcal/(mol x Å^2) – please see Fig S5 (64800 restraints in total). Then another optimisation step was applied allowing cell optimisation but just in Z – direction. The external pressure 10^5 Pa was applied. During this optimisation step the initial shrinkage of the system in Z – direction was obtained. The same method and parameters used as in the first optimisation step just with the exception of the maximum number of optimisation steps which was here set to 20 000. At the end, the preprocessed molecular systems were simulated using Molecular Dynamics (naturally still with above described Si-Si distance restraints) but now in NPT ensemble (T = 298 K, P = 10^5 Pa, Nosé-Hoover thermostat and Parrinello-Rahman barostat used) for 70 ps which was enough for obtaining well equilibrated systems [7]. The time step had to be reduced here to 0.25 fs to ensure stability of the MD algorithm in presence of restraints. During this final equilibration the simulated system (box) was allowed to change in all 3 axes and also in all 3 angles. We repeated this last simulation part 3x for all the cases, starting from the same preprocessed structure, to have better data representation for each case. Since starting structure was identical in all 3 final NPT simulations, thermostat and barostat are deterministic the different MD trajectories were caused by the different starting velocities which are generated randomly according to Maxwell–Boltzmann distribution.The precise *d*-spacing values were then obtained based on simulated X-ray analysis which was done using Reflex module from Materials Studio. Just the last frame of each MD trajectory was analysed as we found in few selected test cases that the dispersion of this quantity among several MD trajectory frames near the end of the trajectory was negligible. So the resulting *d*-spacing value for the given D/Mt case was calculated as the average over the *d*-values obtained by analysis of the last frames of all 3 MD trajectories. The same holds for energetic analyses.

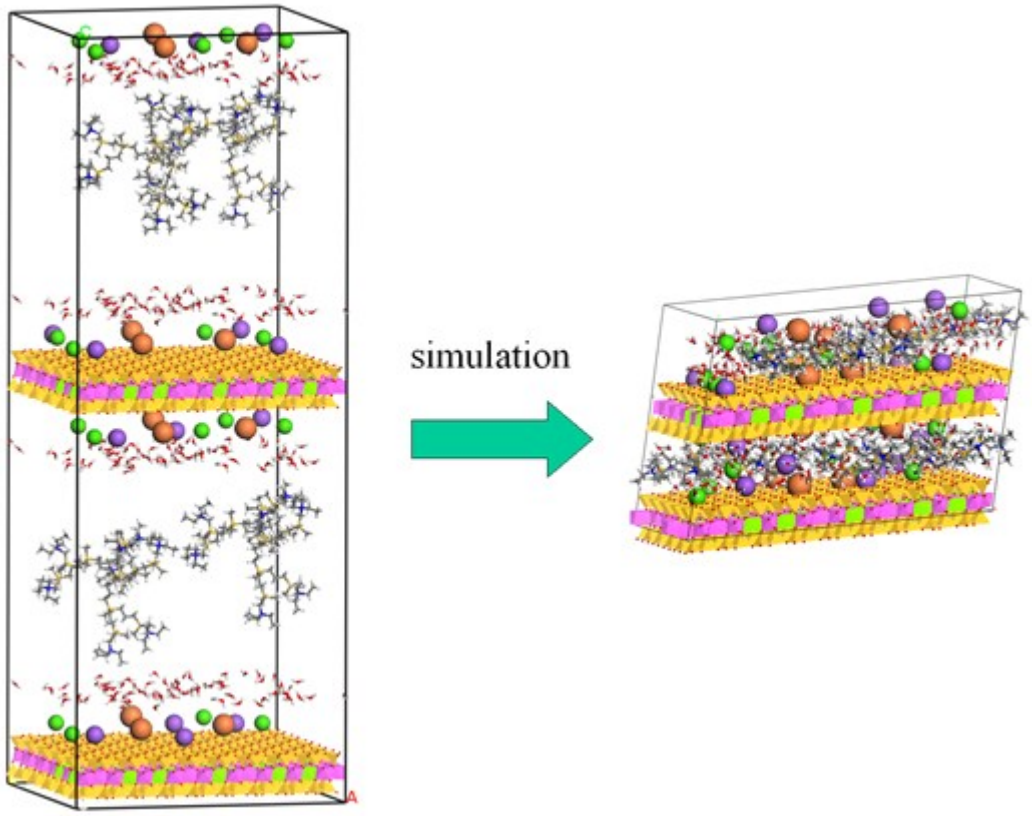

Figure S4. Example of the initial (LEFT) and the final (RIGHT) configuration of simulated **D2Mt** system containing two silicate layers, Na+,K+,Ca++ cations, water molecules and two dendrimers of the second generation. **Mt** layers are in polyhedron representation. Colours: Si – yellow, Al – magenta, Mg and Ca++- green, O - red, H - white, C - gray, N - blue, Na+ - purple , K+ - orange.

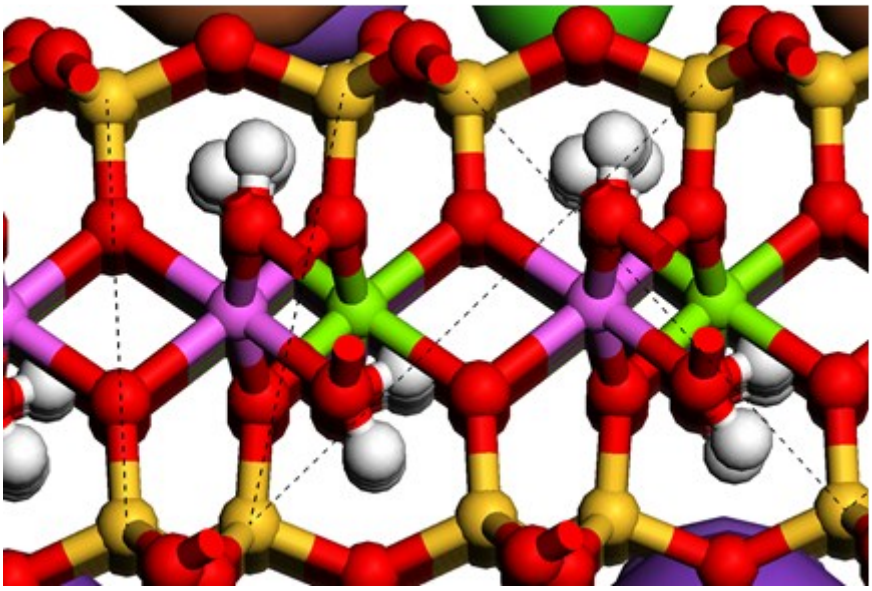

Figure S5. Illustration of the restrained Si-Si distances between Si atoms from the opposite Si layers. Just few restrained distances indicated (thin black dashed lines). Colour coding of the atoms within the **Mt** layer. Si – yellow, Al – magenta, Mg – green, O – red, H – white.

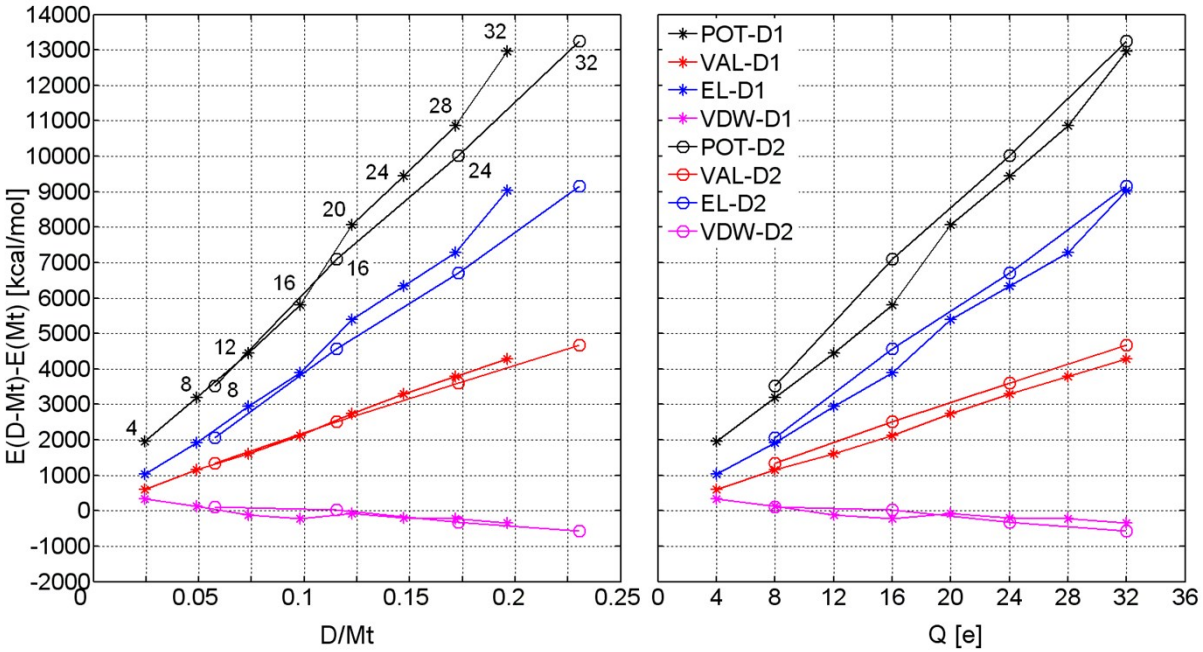

Figure S6. Difference between the potential energy of the dendrimer-montmorillonite system E(D-Mt) and potential energy of the pure (hydrated) montmorillonite E(Mt) as the function of the mass ratio of dendrimers inside the Mt interlayer space and Mt (left) and as the function of exchanged (dendrimer) charge per one modelled Mt layer (right). VAL – valence contribution (bond + angle + torsion terms), EL – electrostatic contribution, VDW – Van der Waals contribution, POT – total potential energy (VAL+EL+VDW). The numbers inside the graph on the left part of fig. 6 denotes exchanged charge [e] per one modelled Mt layer.

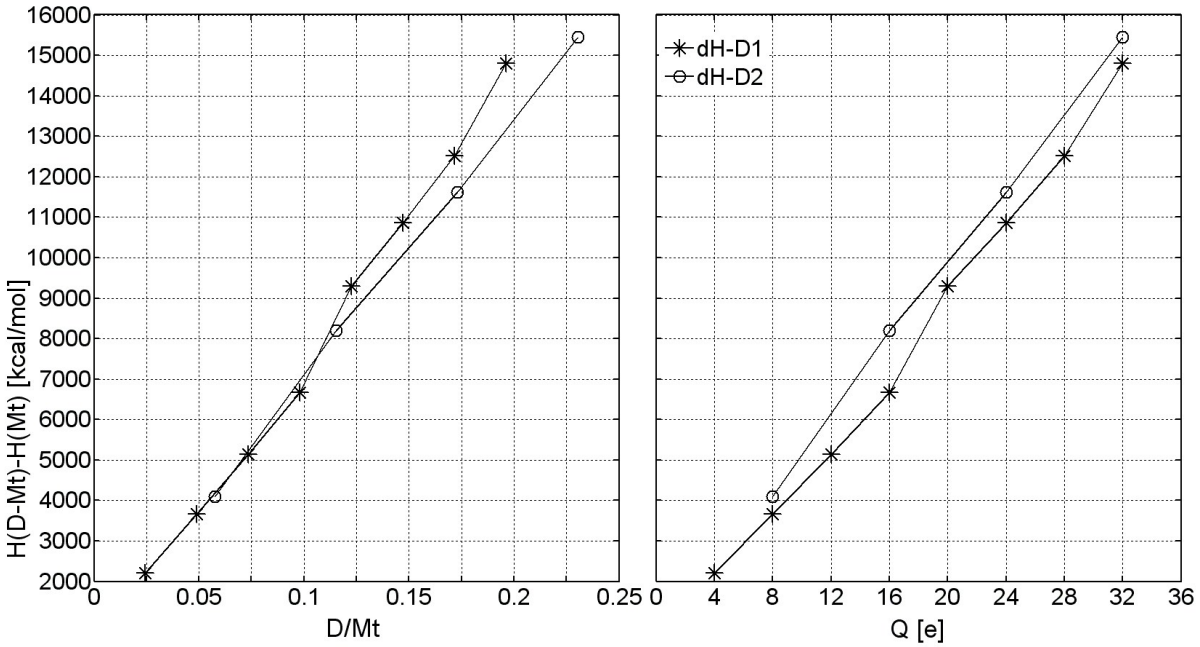

Figure S7. Difference between the enthalpy of the dendrimer-montmorillonite system H(D-Mt) and enthalpy of the pure (hydrated) montmorillonite H(Mt) as the function of the mass ratio of dendrimers inside the Mt interlayer space and Mt (left) and as the function of exchanged charge per one modelled Mt layer (right).

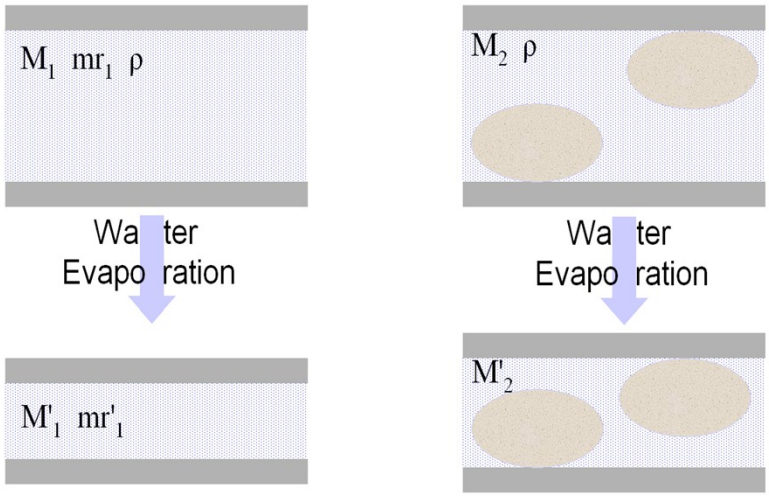

$M'_1 = M_1 * mr'_1 / mr_1$

$M_2 = M_1 - N_D * V_D * \rho$

$M'_2 = M_2 * mr'_1 / mr_1 = M'_1 - mr'_1 / mr_1 * N_D * V_D * \rho$

Figure S8. Illustration of the water content (mass M'_2) estimation in case of simulated D-Mt systems - see molecular modelling methods section.

"dE-discussion"

If we look at figure S6 we can see how dE depends on D/Mt (left) and exchanged (dendrimers) charge (right). As we can see in the left side of the fig. S6, the total potential energy "penalty" dE_{POT} seems to be growing quite similarly in both cases (D1-Mt, D2-Mt) up to cca D/Mt = 0.12. For higher D/Mt values dE_{POT} grows faster in case of D1-Mt systems, but it is clearly just the electrostatic component (dE_{EL}) which makes the difference between D1-Mt, D2-Mt cases because both remaining contributions (dE_{VDW}, dE_{VAL}) follow practically identical dependence on D/Mt. The reason of the higher dE_{EL} "penalty" in case of D1-Mt systems could be partly explained just by the fact that at the given D/Mt value there will be always higher exchanged (dendrimer) charge in case of D1-Mt system because charge of the given mass m of dendrimer D1 is Q(m, D1) = 4*m/m(D1) and charge of the same mass m of dendrimer D2 is $\underline{Q(m, D2)}$ = 8 * m/m(D2) = 8 * m/(2.351 * m(D1)) = 3.4 * m/m(D1) = 3.4 * Q(m, D1)/4 = $\underline{0.85*Q(m, D1)}$ where 2.351 is the ratio m(D2)/m(D1). Therefore at the given D/Mt value the exchanged charge in D1-Mt system is always 4/3.4 = 1.176 times higher than in case of D2-Mt which also means that comparing to D1-Mt system, in D2-Mt case there is higher amount of positive charge represented by free cations (Na^+,K^+, Ca^{++}) which can much better/effectively electrostatically interact with Mt platelets and also with internal H_2O molecules (i.e. lower the total electrostatic energy) than dendrimer terminal cationic groups. We can directly compare 7xD1 and 3xD2 cases which have almost identical value of D/Mt. As we can see the dendrimer charge difference is here 28-24 = 4. From the viewpoint of this hypothesis it is unclear why up to ca D/Mt = 0.12 the dE_{EL} and hence also dE_{POT} grows quit similarly for both dendrimers. We may speculate that difference in dE starts to appear from the moment when the charge difference is sufficiently high. As we can see the system 5xD1-Mt is the first case where is evident some deviation from the D2-Mt dependence. At this point is theoretical dendrimer charge difference between D1-Mt and D2-Mt systems almost exactly

equal to 3. Another possible explanation could be the influence of several factors which can eventually cancel each other. If we look at the figure S9 (left), we can see that d-spacing values are first slightly higher for the D2Mt systems and then (for higher D/Mt values) became d-spacing dependence on D/Mt almost identical for D1Mt, D2Mt systems. Higher d-spacing value means higher dE penalty (worse mutual interaction of platelets) and it is also evident from the fact that d grows with D/Mt as well as dE. So in the first part of the dE(D/Mt) dependence, D2 is energetically slightly disfavoured thanks to slightly higher d values but at the same time it has small advantage of higher amount of cations. Induced energy effects may eventually nearly cancel each other as confirmed by the nearly identical dE(D1/Mt) , dE(D2/Mt) dependencies for low D/Mt ratios (see fig. S6). For higher D/Mt values differences between *d*(D1/Mt) and *d*(D2/Mt) are vanishing while difference in exchanged (dendrimer) charge is growing which results in faster growing of the dE_{EL} and hence also dE_{POT} in D1-Mt case. If we check the right side of the figure S6 we may see dE dependence on the exchanged (dendrimers) charge. As we can see the D1Mt and D2Mt systems differ here slightly in dE_{VAL} , dE_{EL} contributions and so also in total dE_{POT}. If we again compare with Figure S9 (right side) we can conclude that the diference between dE_{POT} (Q) for D1-Mt, D2-Mt systems is determined by differences in *d*(Q). For example for Q = 8 *d*(D1) is very close to *d*(D2) which results in close values of dE_{POT}(Q, D1), dE_{POT}(Q, D2). On the other hand when Q = 16, *d* is significantly higher in D2 case and we can see that this induces also the highest difference between the dE_{POT}(Q, D1), dE_{POT}(Q, D2). Interestingly at Q = 32 the dE_{POT}(Q, D1), dE_{POT}(Q, D2) values are again almost identical (as in the case Q = 8) in spite the fact that difference in d for this charge is 1.33 Å. This difference in case of big (ca 20 Å) *d* value is probably too small to cause higher difference in dE. So there seems to be no reason to assume that D2 is able to interact inside the interlayer space with Mt platelets significantly better than D1 of the same/similar amount. From the point of the potential energy or enthalpy there seems to be no explanation of the experimentally observed fact that bigger D2 intercalates Mt in significantly higher amount (mass, charge) than it is in case of smaller D1.

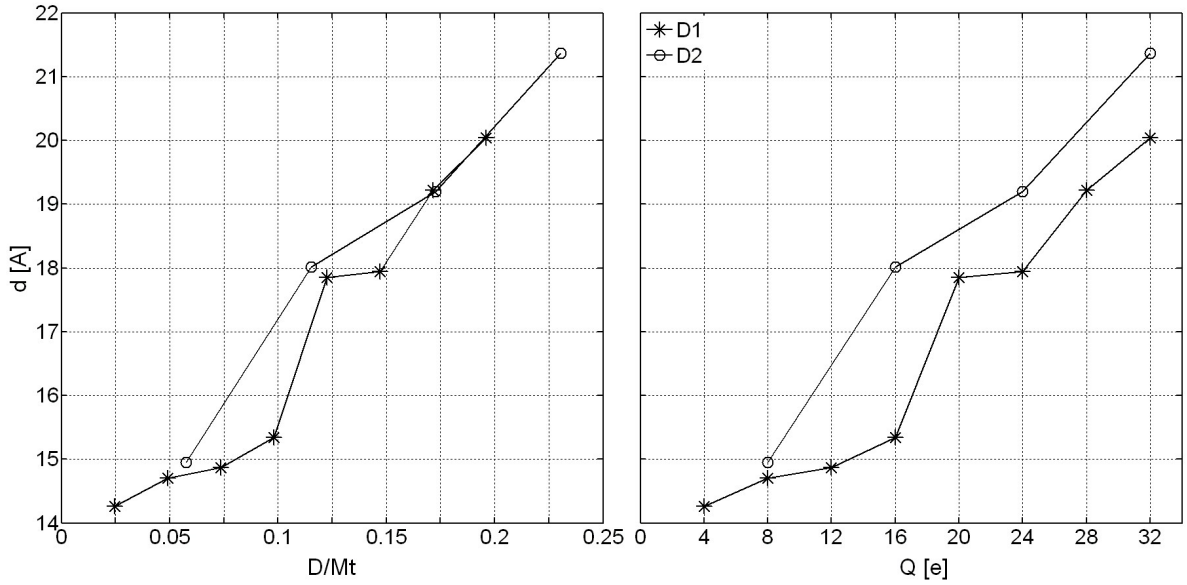

Figure S9. Calculated d-spacing as the function of the mass ratio of dendrimers inside the Mt interlayer space and Mt (left) and as the function of exchanged (dendrimer) charge per one modelled Mt layer (right).

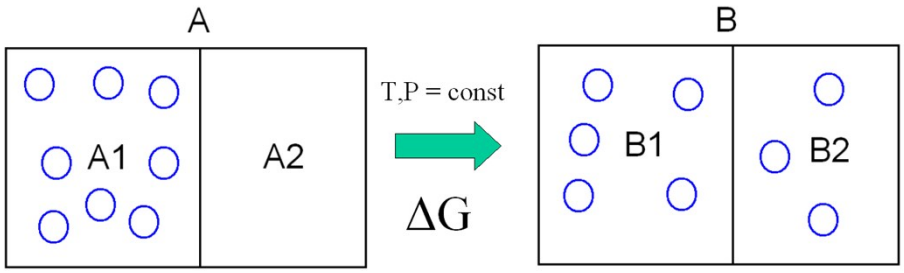

$\mathbf{\Delta G} = G_B - G_A$

$\mathbf{G_A} = H_A - TS_A$

$\mathbf{H_A} = E^{pot}_A + E^{kin}_A + PV_A = E^{pot}_{A1} + E^{pot}_{A2} + E^{pot}_{A1/A2} + E^{kin}_{A1} + E^{kin}_{A2} + P(V_{A1} + V_{A2})$

$\mathbf{S_A} = S_{A1} + S_{A2}$

The same for **B** then :

$\mathbf{\Delta G} = E^{pot}_{B1} - E^{pot}_{A1} + \mathbf{E^{pot}_{B2} - E^{pot}_{A2}} + E^{pot}_{B1/B2} - E^{pot}_{A1/A2} + E^{kin}_{B1} - E^{kin}_{A1} +$
$+ \mathbf{E^{kin}_{B2} - E^{kin}_{A2}} + P(V_{B1} - V_{A1}) + \mathbf{P(V_{B2} - V_{A2})} - T(S_{B1} - S_{A1}) - T(S_{B2} - S_{A2})$

(If also N = const then: $E^{kin}_{B1} - E^{kin}_{A1} + E^{kin}_{B2} - E^{kin}_{A2} = 0$)

Figure S10. Free energy change connected with transition of the system from state A into state B. For spontaneous transition $\Delta G < 0$. G – free Gibbs energy, H – enthalpy, T – temperature, P – pressure, S – entropy, E^{pot} – potential energy, E^{kin} – kinetic energy, $E^{pot}_{X1/X2}$ - part of the potential energy which comes from interactions between parts X1 and X2, N – total number of particles. Lets interpret A as the initial solution containing water+dendrimers (A1) and pristine Mt (A2) and B the same system after some time during which some dendrimers leave water so we get less concentrated dendrimer-water solution B1, and are transferred into Mt so we get D-Mt system (B2). Then the analysed/discussed energetic penalty $dE = (E^{pot}_{B2} – E^{pot}_{A2})$ and eventually whole enthalpic penalty $dH = dE + E^{kin}_{B2} - E^{kin}_{A2} + P (V_{B2}-V_{A2})$.

References :

[1] A. Viani, A. Gualtieri and G. Artioli, *American Mineralogist*, 2002, **87**, 966–975, www.crystallography.net/cod/9002779.html

[2] A. K. Rappe and W. A. Goddard, *J. Phys. Chem.*, 1991, **95**, 3358-3363.

[3] L. Sun, J. T. Tanskanen, J. T. Hirvi, S. Kasa, T. Schatz and T. A. Pakkanen, *Chemical Physics,* 2015, **455**, 23–31

[4] J. W.Chu, B. L.Trout and B. R. Brooks, *J. Chem. Phys.*, 2003, **119**, 12708-12717

[5] N. Karasawa and W. A. Goddard, J. Phys. Chem., 1989, 93, 7320–7327.

[6] S. Nosé, *J. Chem. Phys.*, 1984, **81**, 511-519.

[7] G. J. Martyna, D. J. Tobias and M. L. Klein, *J. Chem. Phys.*, 1994, **101**, 4177–4189.

[8] R. K. Hawkins and P. A. Egelstaff, *Clays and Clay Minerals*, 1980, **28**, 19-28.

[9] R. Torrence Martin, *Clays and Clay Minerals,* 1960, **9**, 28-70.